Check for updates

View Article Online
View Journal

Analyst

Accepted Manuscript

This article can be cited before page numbers have been issued, to do this please use: J. Xu, K. Xu, Y. Han, D. Wang, X. Li, T. Hu, H. Yi and Z. Ni, *Analyst*, 2020, DOI: 10.1039/D0AN00681E.

This is an Accepted Manuscript, which has been through the Royal Society of Chemistry peer review process and has been accepted for publication.

Accepted Manuscripts are published online shortly after acceptance, before technical editing, formatting and proof reading. Using this free service, authors can make their results available to the community, in citable form, before we publish the edited article. We will replace this Accepted Manuscript with the edited and formatted Advance Article as soon as it is available.

You can find more information about Accepted Manuscripts in the Information for Authors.

Please note that technical editing may introduce minor changes to the text and/or graphics, which may alter content. The journal's standard Terms & Conditions and the Ethical guidelines still apply. In no event shall the Royal Society of Chemistry be held responsible for any errors or omissions in this Accepted Manuscript or any consequences arising from the use of any information it contains.

ROYAL SOCIETY OF CHEMISTRY

rsc.li/analyst

Please do not adjust margins

View Article Online
DOI: 10.1039/D0AN00681E

ARTICLE

3D Porous Graphene Aerogel@GOx Based Microfluidic Biosensor for Electrochemical Glucose Detection†

Jian Xu, [a] Kangkai Xu, [a] Yu Han, [a] Di Wang, [a] Xiao Li, [a] Tao Hu, *[a] Hong Yi *[a] and Zhonghua Ni *[a]

As a chronic disease, diabetes may result in serious complications that endanger the health and life of patients. Accurate and real-time detection of blood sugar levels is of great significance for the prevention and treatment of diabetes. In this paper, an enzymatic electrochemical microfluidic biosensor for glucose detection was developed based on three-dimensional (3D) porous graphene aerogel and glucose oxidase (GOx). The graphene aerogel was prepared by freeze-drying graphene hydrogel and has a high electrical conductivity, the 3D porous structure provided a good near-biological condition for GOx and the increased specific surface area allowed more GOx to be immobilized on the graphene aerogel. The microfluidic system greatly reduced the consumption of samples during tests. Amperometric measurements were carried out to test glucose concentrations, and the enzyme biosensor showed a liner range from 1 mM to 18 mM (R = 0.991). The limit of detection (LOD) was 0.87 mM (S/N = 3) and the sensor showed excellent selectivity and stability. Finally, monitor of glucose in serum samples was achieved by the proposed sensor and the good recoveries were obtained. Due to its excellent performance, the proposed biosensor has a favorable application prospect in the prevention and clinical diagnosis of diabetes. Furthermore, our method, which is to prepare the graphene aerogel modified electrode in a microfluidic chip, can be widely used in various electrochemical sensors.

Received 00th January 20xx,
Accepted 00th January 20xx

DOI: 10.1039/x0xx00000x

Published on 05 June 2020. Downloaded on 6/6/2020 2:33:00 AM.

1. Introduction

Abnormal blood glucose level in humans will trigger serious diseases,[1,2] the most common of which is diabetes. As a chronic disease, diabetes can cause serious complications that endanger the health and life of patients.[3] At present, the number of diabetic patients is increasing.[4] Accurate and real-time determination of glucose level is of great significance to the treatment of diabetes. The detection of glucose with conventional analytical instruments like high performance liquid chromatography (HPLC),[5,6] capillary zone electrophoresis (CZE)[7,8] and gas chromatography (GC)[9,10] is accurate and reliable, but these methods rely on expensive instruments and complex operation. Therefore, a variety of electrochemical sensors for glucose detection have been developed, which can mainly be divided into two categories: enzymatic-based sensors and non-enzymatic sensors.[11]

As to non-enzymatic glucose sensors, which usually utilize metal,[12,13] and metal nanomaterials[14-17] as electrodes, they exhibit good sensitivity and low limit of detection (LOD). However, the selectivity for glucose detection with these sensors seems to be unsatisfactory and the sensors' electrodes have possibility of being interfered by proteins, chlorides ions and other species, which limit their application in practical monitoring glucose.

Enzymatic-based methods, which immobilize enzymes on sensors, achieve the determination of glucose level by detecting the product (such as H_2O_2) of catalytic oxidation of glucose or directly exploring the process of catalytic reactions. Electrochemical enzymatic-based sensors for glucose detection, particularly amperometric GOx-based sensors have been widely studied and commercialized since 1962,[18,19] and have played a dominant role in simple, fast, easy-to-use blood sugar monitoring,[20,21] for their high sensitivity, wide linear range, excellent selectivity, low cost and low LOD. However, compared to other methods, despite amperometric GOx-based sensors' unparalleled advantages and being extensively applied in practical glucose detection, one of the non-ignorable drawbacks of these enzymatic-based methods is the difficulties for immobilization of high active enzymes,[20] external environmental factors (like temperature, pH and humidity)[22] and instability originating from the nature of enzymes may result in the reduction of enzymes activity,[23-25] which will affect the accuracy of detection systems. Thus, reliable means to immobilize enzymes and maintain their activity are expected to improve the performance of enzyme sensors and improve their reutilization.

[a] School of Mechanical Engineering, and Jiangsu Key Laboratory for Design and Manufacture of Micro–Nano Biomedical Instruments, Southeast University, Nanjing 211189, China.
* Corresponding authors: hutao@seu.edu.cn; yihong@seu.edu.cn; nzh2003@seu.edu.cn.
† Electronic Supplementary Information (ESI) available. See DOI: 10.1039/x0xx00000x

Analyst Accepted Manuscript

View Article Online DOI: 10.1039/D0AN00681F

Published on 05 June 2020. Downloaded on 6/6/2020 2:33:00 AM.

Hence, we combined 3D porous graphene aerogel with GOx in microfluidic system to prepare a new biosensor for accurate electrochemical detection of glucose. The 3D porous graphene aerogel was prepared by freeze-drying graphene hydrogel, which was gained through in situ chemical reduction of graphene oxide by L-ascorbic acid. In addition to its high electrical conductivity, simple synthesis and low cost,[26] the porous structure of this prepared 3D graphene aerogel greatly increased the specific surface area, which meant that more GOx could be modified on graphene and thus the sensitivity of the sensor was increased. On the one hand, the graphene aerogel provided good physiological conditions for GOx, on the other hand, its 3D porous structure made GOx well wrapped in a graphene aerogel, which avoided contamination of GOx. Both were good for maintaining enzyme activity and improving the stability and reutilization of the sensor.

In our detection system, the accurate determination of glucose level was achieved through amperometric measurement of hydrogen peroxide (H_2O_2), the product of catalytic oxidation of glucose by GOx. Due to the specificity of GOx for glucose, the selectivity of our sensor for glucose detection was quite satisfactory. Furthermore, the potential used during our detection process was relatively low (-0.3 V), which was critical for detection.[27] Relatively low potential restrained the reduction of other substances (such as ascorbic acid (AA), uric acid (UA), etc.) when detecting H_2O_2 (the product of catalytic oxidation of glucose) with our sensor, which further improved the selectivity and accuracy of the sensor. In addition, the dimensions of the sensor was designed to be very small to form a microfluidic chip, which meant the reduction of sample consumption (less than 3 μL) and the sensor manufacturing cost. Therefore, the proposed low-cost, excellent performance enzyme-based sensor is expected to be well applied in practical situations such as large-scale screening of diabetes and self-management of diabetics.

2. Experimental section

2.1 Reagents and materials

All chemicals were analytical grade. Methanol, absolute ethanol, H_2SO_4, $KMnO_4$ and $NaNO_3$ were purchased from Sinopharm Chemical Reagent Co.,Ltd (Shanghai, China). N-(3-dimethylaminopropyl)-N'-ethylcarboiimide hydrochloride (EDC), N-hydroxysulfosuccinimide (NHS), glucose oxidase (GOx), fructose, maltose, sucrose and lactose were purchased from Aladdin (Shanghai, China). Uric acid (UA), glucose and 1-pyrenecarboxylic acid (PCA) were purchased from Sigma-Aldrich (St. Louis, USA). Ascorbic acid (AA) was purchased from Alfa Aesar (Shanghai, China) and silver conductive paint was purchased from Mechanic (Hong Kong, China). ITO glass (thickness of ITO film: 185 nm; square resistance: ≤6 Ω) was customized by South China Xiangcheng Technology (Hunan, China).

2.2 Fabrication of the microfluidic biosensor

As it is shown in Supplementary Fig. S1a, the proposed sensor consists of four parts, including ITO glass, 3D graphene, microchannel and PDMS cover. The dimensions of the custom ITO glass and the dimensions of the microchannel are shown in Fig. S1b and S1c, respectively. The microchannel was obtained by spin-coating PDMS on a polyimide film and drying, followed by laser processing. It is only 50 μm in height, which means the detection system is extremely small and the sample consumption is greatly reduced. The preparation process of the biosensor was described below.

First, microchannel was bonded to ITO glass through a plasma treatment and a thin layer of conductive silver paste was applied to the specific part of ITO to enhance the adhesion of ITO to graphene. Second, 4 mL graphene oxide solution (5 mg/mL, prepared through the modified Hummers' method[28]) was mixed with AA and then 1 mL PCA/methanol suspension (3 mg/mL) was added to the mixture. 10 μL of the mixture was evenly dropped onto the silver paste, then the chip was heated in 40℃ water bath for 16 h. The chip was immersed in ultrapure water with low-speed magnetic stirring for 1 h to remove residual AA, and water droplets on the chip surface was blown out with nitrogen. Third, the chip was kept in the refrigerator at -20℃ for 48 h and then was freeze-dried to obtain 3D graphene structure. Fourth, the carboxyl groups of PCA was activated by EDC and NHS, then 20 μL GOx (50 mg/mL) was spread onto the activated graphene and the chip was incubated at 0℃ for 12 h. Last, the chip was encapsulated with PDMS cover. (Before bonding, only PMDS cover needed plasma treatment, while the microchannel just needed to tear off the polyimide film on it.) The complete chip is shown in Fig. 1a.

2.3 Chronoamperometry (CA) detection of glucose

Chronoamperometry (CA) was used to detect glucose to obtain its calibration curve. First, 3 μL PBS without glucose was injected into the sensor by continuous syringe pump at a speed of 15 μL·min^{-1} and the current of the system was recorded using CA (potential: -0.3 V). Then 3 μL PBS with glucose was injected into the sensor in the same way. After 15 min, the system current was determined again with CA at voltage of -0.3 V.

Before the reuse of the sensor, ultrapure water was used to clean the sensor by continuous syringe pump at a speed of 15 μL·min^{-1} for 2 min.

2.4 Instrumentation and measurements

Scanning electron microscopy (SEM, Helio NanolabTM 600i, FEI Company, America) and Raman spectroscopy measurements (Alpha 300 Raman-AFM, Witec, Germany) were used to observe the morphology of the proposed 3D graphene sample. X-ray diffraction system (XRD, D8-Discover, Bruker, Germany) was used to analyze the composition of the sample. The cyclic voltammetry (CV) and chronoamperometry (CA) were conducted on the electrochemical workstation (CHI660E, Chenhua, Shanghai, China) with a three electrode configuration containing a working electrode of the graphene modified indium tin oxide (ITO), a reference electrode of Ag/AgCl and a counter electrode of ITO (more details about the electrodes can be seen in Fig. S2).

3. Results and discussion

Analyst Accepted Manuscript

This journal is © The Royal Society of Chemistry 20xx

View Article Online
DOI: 10.1039/D0AN00681F

Published on 05 June 2020. Downloaded on 6/6/2020 2:33:00 AM.

3.1 Characterization of graphene aerogel modified electrode

Graphene aerogel's 3D porous structure can immobilize more GOx on graphene electrode and maintain enzyme activity, which can improve the sensitivity and stability of sensor. As described in experimental section 2.2, we successfully obtained graphene hydrogel though in situ chemical reduction of graphene oxide, and freeze-dried the hydrogel to prepare 3D porous graphene aerogel. In order to verify the successful synthesis of graphene aerogel and its 3D porous structure, the graphene electrode was characterized by SEM, Raman spectroscopy and XRD. Fig. 1b is the SEM image of the graphene samples, manifesting the 3D porous structure of graphene aerogels. The Raman spectroscopy of the samples is shown in Fig. 1c. Two strong bands D (1349.69 cm^{-1}) and G (1580.26 cm^{-1}), which are well known for graphene, and two weak, broad bands D' and G' were all observed. The results are consistent with previous work about 3D graphene aerogels,[29,30] manifesting a similar 3D structure and defect density.[31,32] The 3D porous structure of graphene aerogel can greatly increase the specific surface area. This facilitates the immobilization and protection of the enzyme and allows the electrode to be in better contact with the detection liquid, which can thereby improve the performance of the sensor. XRD spectra results are shown in Fig. 1d. A weak, broad diffraction peak (002) appears at 25.5° (2θ) indicates the successful synthesis of graphene and that graphene aerogel is a multilayer structure rather than a single layer planar structure.[32] In the figure, no diffraction peak appears between 10 and 20 degrees, indicating the perfect reduction of oxygen-containing functional groups of graphene oxide.

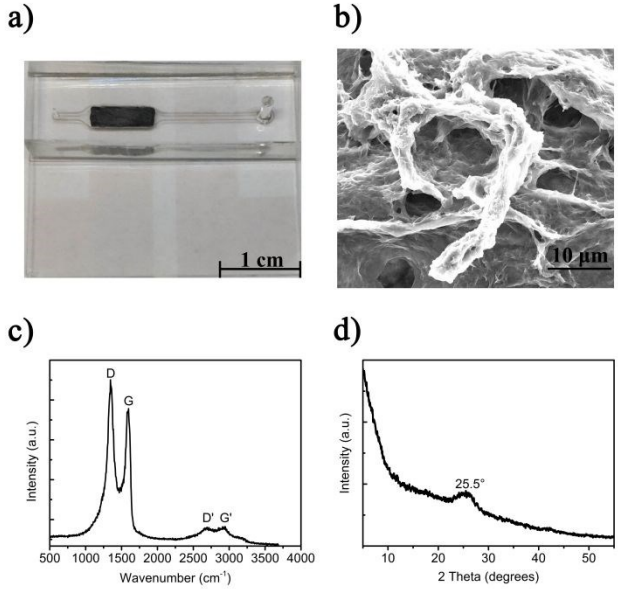

Fig. 1 (a) The image of the proposed biosensor. (b) SEM image of 3D graphene aerogel. (c) Raman spectroscopy of 3D graphene aerogel. (d) XRD spectra of 3D graphene aerogel.

3.2 Validation of sensing principle and Optimization of the graphene aerogel biosensor

Scheme 1 elaborates the detection platform and the sensing principle of our proposed biosensor. When glucose is injected into the biosensor, it is catalytically oxidized by GOx immobilized on the 3D graphene electrode into gluconolactone and H_2O_2. Graphene has certain electrocatalytic ability to H_2O_2,[24] which means the current of electrochemical system based on graphene electrode will change because of the existence of H_2O_2. Thus the level of glucose can be indirectly determined by measuring its product H_2O_2 based on the change of current in the electrochemical system. In order to verify the sensing principle of our biosensor, detection of H_2O_2 with the proposed sensor was firstly conducted.

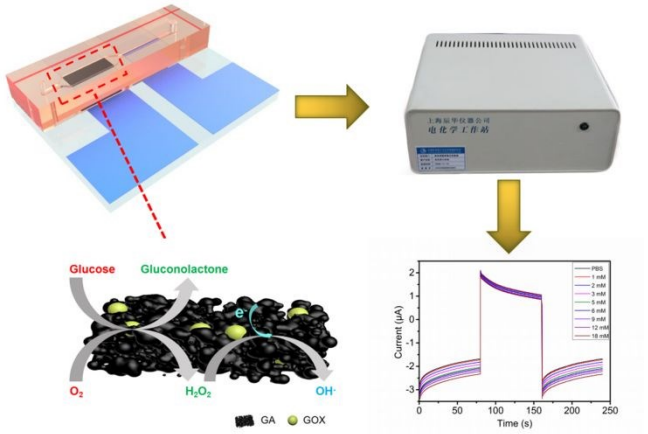

Scheme 1 Schematic illustration of electrochemical glucose detection using the proposed 3D porous graphene aerogel@GOx based microfluidic biosensor.

Measurements of H_2O_2 under macroscopic conditions for verifying the feasibility of the sensing principle were conducted firstly. Fig. S3 shows the Cyclic voltammetry (CV) curves of the 3D graphene electrode immersed in PBS in presence and absence of 3mM H_2O_2. As shown in Fig. S3, the 3D graphene electrode immersed in PBS with 3mM H_2O_2 exhibits an obvious increase in cathodic reduction peak compared to that without H_2O_2. According to the literature,[33,34] the mechanism for H_2O_2 electro-reduction can be described by the following equations.

$$H_2O_2 + e^- \rightarrow OH_{ad} + OH^- \quad (1)$$

$$OH_{ad} + e^- \rightarrow OH^- \quad (2)$$

$$2OH^- + 2H^+ \rightarrow 2H_2O \quad (3)$$

This result proves the 3D graphene's electrocatalytic ability to H_2O_2. In fact, the presence of graphene enhances the reduction of H_2O_2 at negative low potentials,[35,36] which improves the anti-interference capability of the sensor during detection.

In order to further verify the sensor's ability to detect H_2O_2, more experiments were used to optimize the detection potential and measure different concentrations of H_2O_2 on this basis using chronoamperometry (CA). First, 3 μL PBS without H_2O_2 was injected into the sensor by continuous syringe pump and the current of the system was recorded using CA. Then 3 μL PBS with H_2O_2 was injected into the sensor to determine the system current in the same way. Due to the cathodic reduction peak appeared at about -0.2 V (Fig. S3), experiments of detecting 3 mM H_2O_2 at -0.4 V, -0.3 V, -0.2 V and -0.1 V were conducted respectively to determine the optimal detection potential. As shown in Fig. 2a, -0.3 V is chosen as the optimal

Analyst Accepted Manuscript

View Article Online
DOI: 10.1039/D0AN00684E

Published on 05 June 2020. Downloaded on 6/6/2020 2:33:00 AM.

detection potential because the current percentage change at -0.3 V is the largest. Different concentrations of H_2O_2 were detected by the same method at -0.3 V. Fig. 2c shows that the percentage change in current is liner with the logarithm of H_2O_2 as the following equation (4).

$$(I - I_0) / I_0 = 0.83697 + 0.2683 \log_{10}(\text{concentration of } H_2O_2) \quad (4)$$

Where, I is the current of sensor after injecting H_2O_2, and I_0 is the sensor current of PBS without any H_2O_2.

Good linear relationship between H_2O_2 and current response (R^2 = 0.992) illustrates the sensor's ability to detect H_2O_2, verifying the feasibility of the program.

As for the detection of glucose, it is mainly determined by detecting H_2O_2, the product of catalytic oxidation of glucose by GOx. Therefore, a very important factor in the detection is the incubation time after glucose is injected into the sensor. The incubation time was optimized using CA at -0.3 V when 3 mM glucose was injected into the sensor. As shown in Fig. 2b, after 3 mM glucose is injected into sensor, the system current response increases with increasing incubation time and stabilizes at an incubation time of 15 min, thus the incubation time is optimized to 15 min.

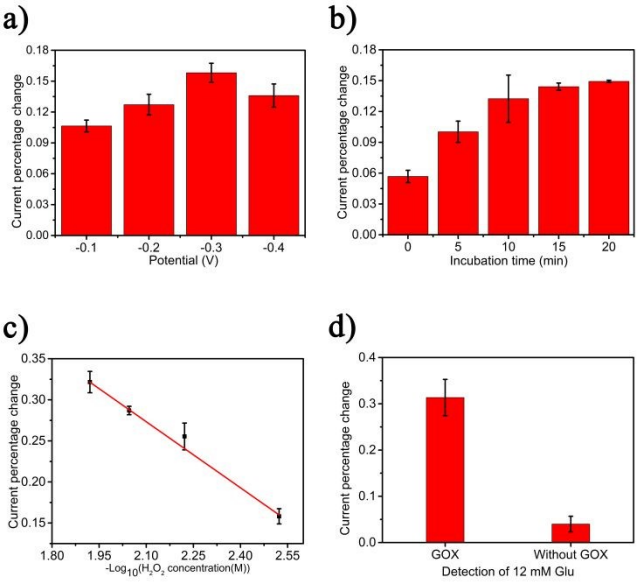

Fig. 2 (a) Current change of the biosensor when 3mM H_2O_2 is injected under voltage conditions of -0.1 v, -0.2 v, -0.3 v and -0.4 V, respectively. (b) Current change of the biosensor when 3mM glucose is injected under different incubation times. (c) Linear plots of the microfluidic biosensor to different concentrations of H_2O_2. (d) Current change of the biosensor when glucose is injected in presence or absence of GOx.

Furthermore, detection of glucose using the sensor without GOx immobilized on the 3D graphene electrode was conducted under the optimal conditions to form a contrast experiment. The results are shown in Fig. 2d. Obviously, compared to that of sensor with GOx, the current response of the sensor without GOx modification is much smaller than that of the sensor with GOx modification, which further validates the correctness of the sensing principle of our enzyme-based sensors.

3.3 Amperometric detection of glucose with the proposed sensor

Our proposed enzymatic electrochemical microfluidic biosensor was used to obtain the calibration plots for glucose concentration detection by measuring different concentrations of glucose in PBS. The measurements were conducted under he optimal conditions determined in 3.2. The biosensors were firstly incubated by different concentrations of glucose for 15 min, and then they were detected with chronoamperometry (CA) (potential: -0.3 V), respectively. Fig. 3 shows the current responses of sensors after incubation by different concentrations of glucose. Obviously, the percentage change in current of the sensor is positively correlated with the glucose concentration. Furthermore, the percentage change in current is liner with the logarithm of glucose concentration as the following equation (5).

$$(I-I_0)/I_0 = 0.83947 + 0.27378 \log_{10}(\text{concentration of glucose}) \quad (5)$$

Where, I is the current of sensor after incubation by glucose, and I_0 is the sensor current of PBS without any glucose.

The sensor's linear range of detection is from 1 mM to 18 mM (R^2 = 0.99) and the limit of detection (LOD) for glucose detection with our sensor is 0.87 mM (S/N = 3). Compared with other glucose biosensors (Table S1), although the proposed sensor does not seem to have an advantage in terms of LOD, the LOD and linear range of the proposed sensor are enough to analyze the glucose in practical situation. (According to 2018 American Diabetes Association (ADA) diagnostic criteria, the normal fasting plasma glucose (FPG) of human is 3.9~5.6 mM. Diabetes is diagnosed as FPG ≥7.0 mM and/or 2-h postprandial glucose (2-h PG) ≥11.1 mM. Prediabetes is defined as FPG ≥5.6 mM and ≤6.9 mM, 2-h PG ≥7.8 mM and ≤11.0 mM.) Furthermore, the proposed sensor consumes much less sample than other sensors.

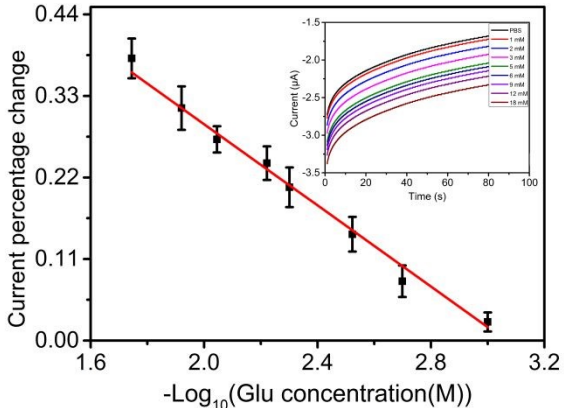

Fig. 3 Linear plots of the microfluidic biosensor to different concentrations of glucose.

3.4 Selectivity and stability of the sensor

As we all know, uric acid (UA), ascorbic acid (AA) and some other substances usually coexist with glucose in human serum.[3] Therefore, it is of great importance to verify the selectivity of the biosensor. AA, UA, lactose, maltose, fructose and sucrose were chosen as interfering substances to evaluate the selectivity of the proposed sensor. The same method was used

Analyst Accepted Manuscript

This journal is © The Royal Society of Chemistry 20xx

Please do not adjust margins

View Article Online
DOI: 10.1039/D0AN00681F

Published on 05 June 2020. Downloaded on 6/6/2020 2:43:00 AM.

to detect these substances, respectively, at a concentration of 12 mM. The result is shown in Fig. 4a. The current response of the sensor to glucose is much greater than those to the interfering species. Since the concentration of glucose is much higher than that of these interfering substances in physiological environment,[37] the selectivity of our sensor is satisfactory. The good selectivity of the sensor can be attributed to the following two points. First, GOx was modified on 3D graphene so that only glucose was oxidized and H_2O_2 was formed during the incubation. Second, due to the low detection potential, only H_2O_2 was consumed during the detection process, while other substances (such as AA, UA, etc.)[38,39] did not participate in the reaction.

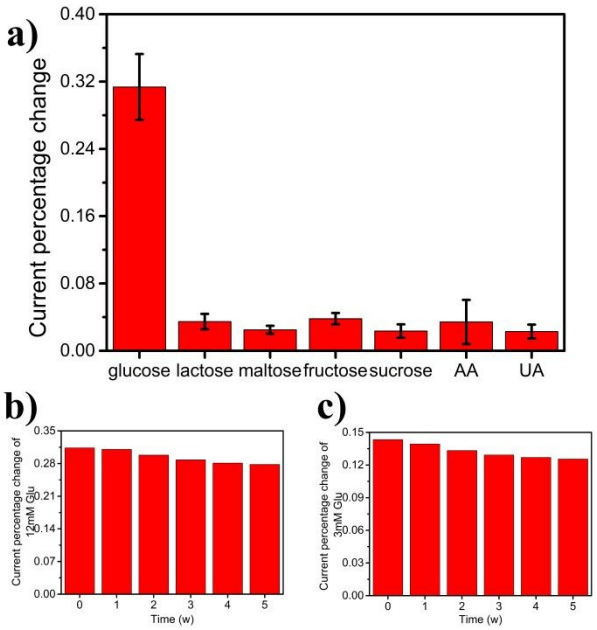

Fig. 4 (a) Current change of the biosensor when glucose and other interfering substances are injected, respectively. Current response of the biosensor after a few weeks to (b) 12mM glucose and (c) 3mM glucose.

Stability is also an important indicator of biosensor performance. The long-term storage stability of 3D porous graphene aerogel@GOx based microfluidic biosensor was examined by storing in the refrigerator at -20℃ and measured at an interval of 1 week. As shown in Fig. 4b and 4c, after five weeks, the current responses of the sensor to 12 mM and 3 mM glucose still retain 89% and 88% of their initial responses, respectively. The results prove that our sensor have favorable stability.

3.5 Real sample analysis

In order to evaluate the performance of the proposed sensor's practical application, the levels of glucose in human serum samples were tested with our sensors. Blood samples were provided by Zhongda Hospital (Nanjing, China) and centrifuged to obtain serum samples. The exact values of the samples were determined by Beckman Coulter LX20 Automatic Biochemical Analyzer in the hospital. The obtained results are listed in Table 1. The recoveries are found to be between 90% and 106% and RSDs are all less than 10%, which indicate that the fabricated sensor has potential in the practical determination of glucose.

Table 1 Results for the determination of glucose in human serum sample.

Samples	Blood glucose (mM)	Found (mM)	Recovery (%)	RSD (%) N = 3
1	6.80	6.29	92.55	2.96
2	5.60	5.81	103.75	4.17
3	8.20	7.67	93.54	5.38
4	4.65	4.21	90.11	3.97
5	10.86	11.51	105.99	7.73

4. Conclusion

An enzymatic electrochemical microfluidic biosensor based on 3D porous graphene aerogel and GOx for glucose detection was developed. Hydrogen peroxide (H_2O_2), the product of catalytic oxidation of glucose by GOx, would lead to current change in the electrochemical system, and thus the determination of glucose could achieved by analyzing the current change in the electrochemical system. 3D porous graphene aerogel was successfully prepared through in situ chemical reduction and freeze-drying method and was characterized by SEM, Raman spectroscopy and XRD to confirm its microstructure. The sensing principle was verified by detecting H_2O_2 and the calibration plots for glucose concentration detection was obtained under the optimal conditions. Due to the specificity of GOx, protection of GOx by 3D structure of graphene aerogel and low detection potential, our biosensor showed good sensitivity and excellent selectivity and stability. Furthermore, the microfluidic biosensor was applied in glucose detection in human serum samples and the recoveries were satisfactory. Therefore, this study puts forward a low cost, good performance and low sample consumption biosensor for glucose detection, which can be potentially developed for practical use.

In addition, the sensor prepared by our method has good biocompatibility, large specific surface area and low sample consumption, thus we believe that this method for preparing a microfluidic biosensor can be of interest in the wider materials chemistry community and can be applied in many related fields.

Conflicts of interest

There are no conflicts to declare.

Acknowledgements

This work was supported by National Natural Science Foundation of China (Grant No. 51605088), by the National Key Scientific Instrument and Equipment Development Project (Grant No.51627808), Natural Science Foundation of Jiangsu Province (Grant No. BK20170667, BK20150600). and the Fundamental Research Funds for the Central Universities (2242016K41022).

Analyst Accepted Manuscript

Please do not adjust margins

Notes and references

1 M. Shao, X. Xu, J. Han, J. Zhao, W. Shi and M. Wei, *Langmuir*, 2011, **27**, 8233-8240.
2 S. Su, Z. Lu, J. Li, Q. Hao, W. Liu, C. Zhu, X. Shen, J. Shi and L. Wang, *New J. Chem.*, 2018, **42**, 6750-6755.
3 W. Meng, Y. Wen, L. Dai, Z. He and L. Wang, *Sensor. Actuat. B-Chem.*, 2018, **260**, 852-860.
4 T. Hu, Y. Ye, K. Chen, F. Long, W. Sang, Y. Zhou, D. Sun and Z. Ni, *Anal. Methods-UK*, 2018, **10**, 5749-5754.
5 J. Ma, X. Hou, B. Zhang, Y. Wang and L. He, *J. Pharmaceut. Biomed.*, 2014, **91**, 24-31.
6 M. P. Gangola, S. Jaiswal, Y. P. Khedikar and R. N. Chibbar, *Food Chem.*, 2014, **154**, 127-133.
7 J. D. Oliver, M. Gaborieau, E. F. Hilder and P. Castignolles, *J. Chromatogr. A*, 2013, **1291**, 179-186.
8 C. Sarazin, N. Delaunay, C. Costanza, V. Eudes and P. Gareil, *Talanta*, 2012, **99**, 202-206.
9 A. Montoya-Arroyo, R. M. Schweiggert, M.-L. Pineda-Castro, M. Sramek, R. Kohlus, R. Carle and P. Esquivel, *Food Hydrocolloid.*, 2014, **35**, 557-564.
10 C. Uri, Z. Juhasz, Z. Polgar and Z. Banfalvi, *Food Chem.*, 2014, **159**, 287-292.
11 A. L. Galant, R. C. Kaufman and J. D. Wilson, *Food Chem.*, 2015, **188**, 149-160.
12 S. Park, T. D. Chung and H. C. Kim, *Anal. Chem.*, 2003, **75**, 3046-3049.
13 Y. Sun, Y. Li, N. Wang, Q. Q. Xu, L. Xu and M. Lin, *Electroanal.*, 2018, **30**, 474-478.
14 Y. Ding, Y. Liu, J. Parisi, L. Zhang and Y. Lei, *Biosens. Bioelectron.*, 2011, **28**, 393-398.
15 C. Li, H. Yamahara, Y. Lee, H. Tabata and J. Delaunay, *Nanotechnology*, 2015, **26**, 305503.
16 G. He, L. Tian, Y. Cai, S. Wu, Y. Su, H. Yan, W. Pu, J. Zhang and L. Li, *Nanoscale Res. Lett.*, 2018, **13**, 3-12.
17 X. Li, K. Ren, M. Zhang, W. Sang, D. Sun, T. Hu and Z. Ni, *Sensor. Actuat. B-Chem.*, 2019, **293**, 122-128.
18 L. Clark and C. Lyons, *Ann. N. Y. Acad. Sci.*, 1962, **102**, 29-45.
19 S. J. Cho, H. B. Noh, M. S. Won, C. H. Cho, K. B. Kim and Y. B. Shim, *Biosens. Bioelectron.*, 2018, **99**, 471-478.
20 J. Wang, *Chem. Rev.*, 2008, **108**, 814-825.
21 W. Mao, B. Cai, Z. Ye and J. Huang, *Sensor. Actuat. B-Chem.*, 2018, **261**, 385-391.
22 R. Wilson and A. P. F. Turner, *Biosens. Bioelectron.*, 1992, **7**, 165-185.
23 T. Hu, J. Xu, Y. Ye, Y. Han, X. Li, Z. Wang, D. Sun, Y. Zhou and Z. Ni, *Biosens. Bioelectron.*, 2019, **136**, 112-117.
24 G. Baskaya, Y. Yildiz, A. Savk, T. O. Okyay, S. Eris, H. Sert and F. Sen, *Biosens. Bioelectron.*, 2017, **91**, 728-733.
25 D. Feng, F. Wang and Z. Chen, *Sensor. Actuat. B-Chem.*, 2009, **138**, 539-544.
26 M. Zhang and Z. Wang, *Appl. Phys. Lett.*, 2013, **102**, 213104.
27 L. Chen, X. Wang, X. Zhang and H. Zhang, *J. Mater. Chem.*, 2012, **22**, 22090-22096.
28 T. Chen, B. Zeng, J. L. Liu, J. H. Dong, X. Q. Liu, Z. Wu, X. Z. Yang and Z. M. Li, *J. Phys.: Conf. Ser.*, 2009, **188**, 012051.
29 G. Tang, Z.-G. Jiang, X. Li, H.-B. Zhang, A. Dasari and Z.-Z. Yu, *Carbon*, 2014, **77**, 592-599.
30 W. Chen, S. Li, C. Chen and L. Yan, *Adv. Mater.*, 2011, **23**, 5679-5683.
31 C. Zhu, T. Y. Han, E. B. Duoss, A. M. Golobic, J. D. Kuntz, C. M. Spadaccini and M. A. Worsley, *Nat. Commun.*, 2015, **6**, 6962-6969.
32 M. A. Worsley, S. Charnvanichborikarn, E. Montalvo, S. J. Shin, E. D. Tylski, J. P. Lewicki, A. J. Nelson, J. H. Satcher, J. Biener, T. F. Baumann and S. O. Kucheyev, *Adv. Funct. Mater.*, 2014, **24**, 4259-4264.
33 R. Liu, S. Li, X. Yu, G. Zhang, S. Zhang, J. Yao, B. Keita, L. Nadjo and L. Zhi, *Small*, 2012, **8**, 1398-1406.
34 F. Meng, X. Yan, J. Liu, J. Gu and Z. Zou, *Electrochim. Acta*, 2011, **56**, 4657-4662.
35 Y. Qin, J. Cui, Y. Zhang, Y. Wang, X. Zhang, H. Zheng, X. Shu, B. Fu and Y. Wu, *Sci. Bull.*, 2016, **61**, 473-480.
36 Y. Lin, F. Lu, Y. Tu and Z. Ren, *Nano Lett.*, 2004, **4**, 191-195.
37 L. Shi, X. Zhu, T. Liu, H. Zhao and M. Lan, *Sensor. Actuat. B-Chem.*, 2016, **227**, 583-590.
38 E. Nossol and A. J. G. Zarbin, *Adv. Funct. Mater.*, 2009, **19**, 3980-3986.
39 P. A. Fiorito and S. I. Córdoba de Torresi, *J. Electroanal. Chem.*, 2005, **581**, 31-37.

View Article Online DOI: 10.1039/D0AN00681E

Published on 05 June 2020. Downloaded on 6/6/2020 2:43:00 AM.

Analyst Accepted Manuscript

This journal is © The Royal Society of Chemistry 20xx